

FIG. 1

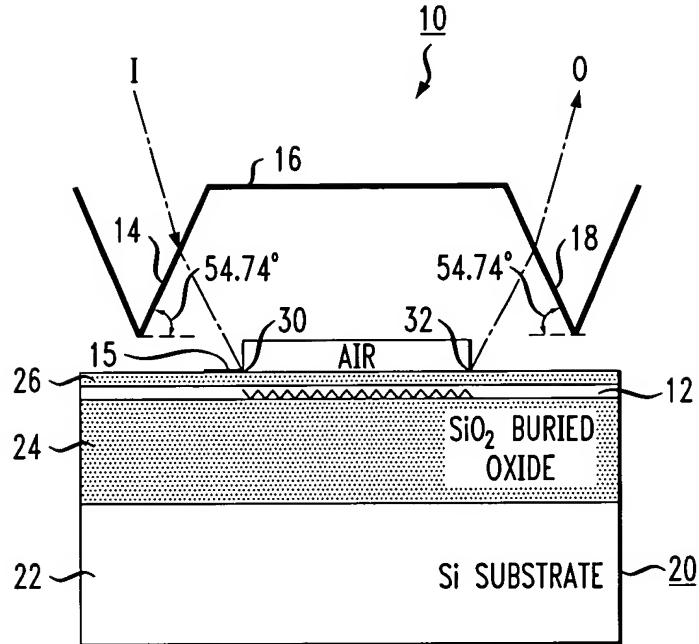
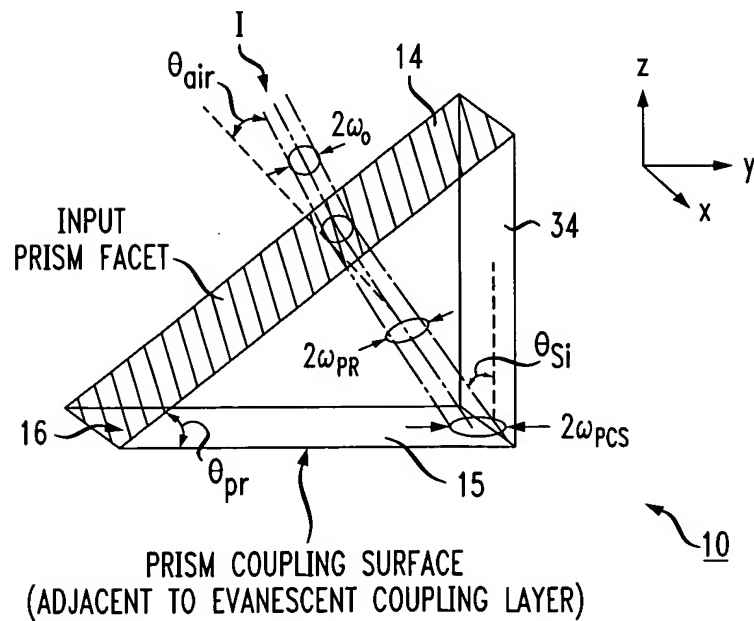


FIG. 2



2/17

*FIG. 3*

WAVELENGTH DEPENDENCE OF BEAM ANGLE INSIDE PRISM ( $\theta_{Si}$ ) AS A FUNCTION OF WAVELENGTH, FOR THREE DIFFERENT WAVEGUIDE THICKNESSES

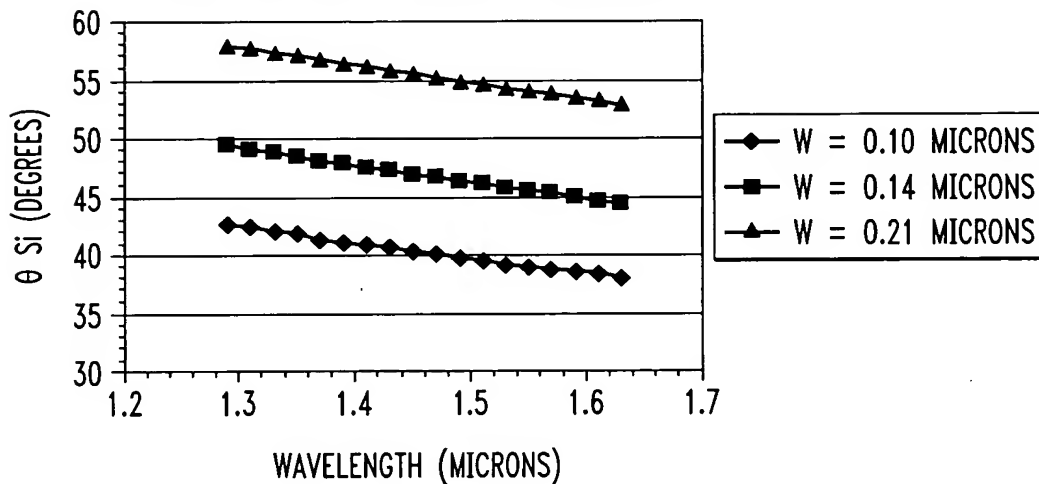
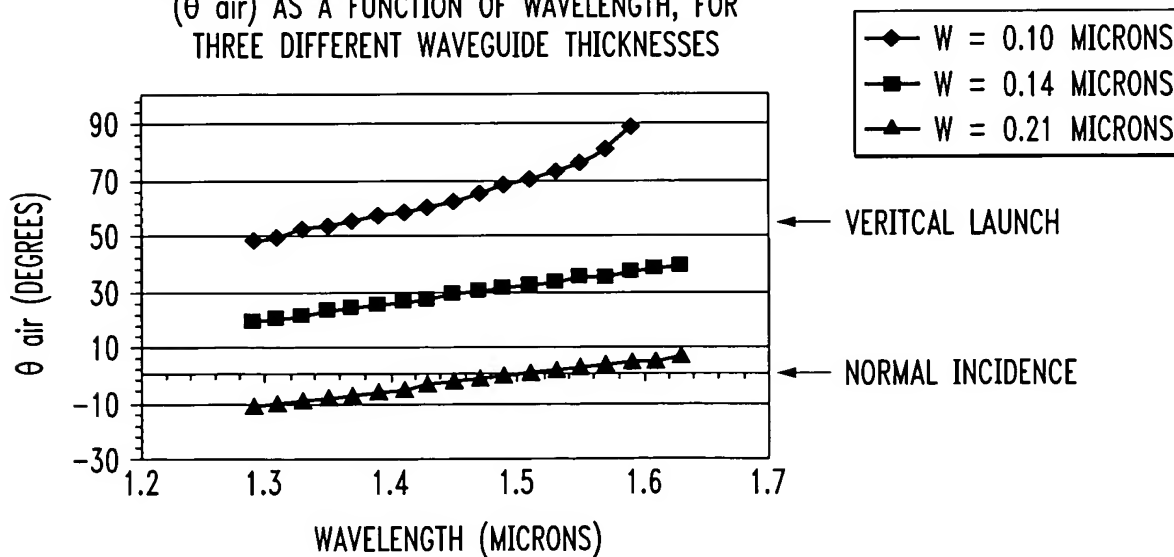


*FIG. 4*

WAVELENGTH DEPENDENCE OF BEAM ANGLE IN AIR ( $\theta_{air}$ ) AS A FUNCTION OF WAVELENGTH, FOR THREE DIFFERENT WAVEGUIDE THICKNESSES



3/17

FIG. 5

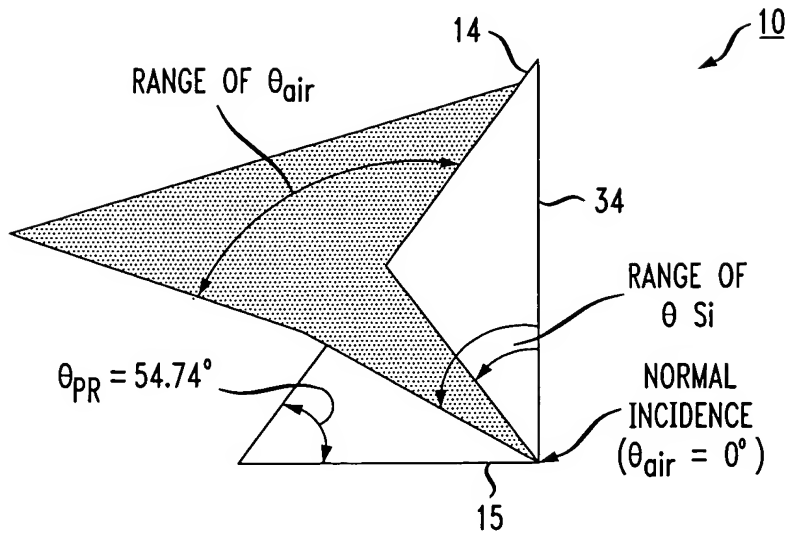
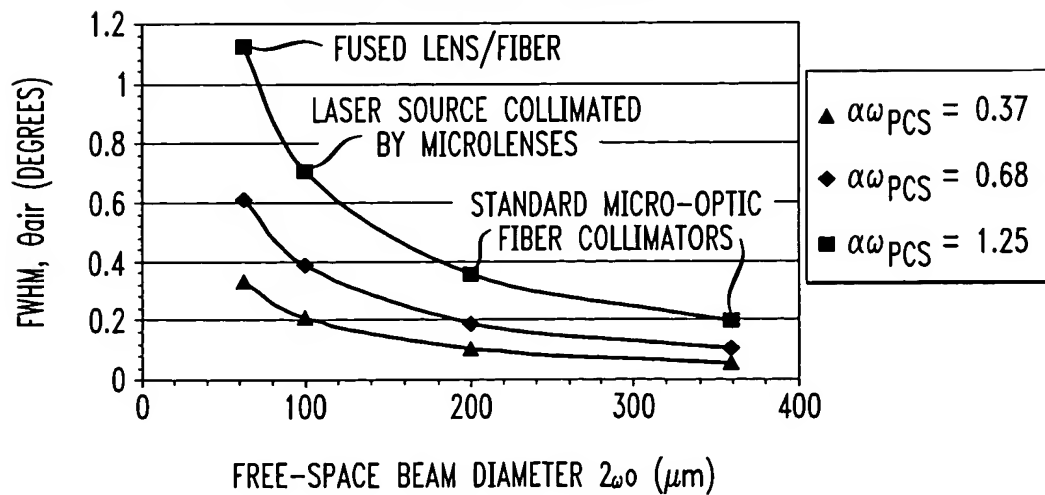


FIG. 6

FREE-SPACE ANGULAR SEPARATION BETWEEN THE 3 dB POINTS (FWHM ( $\theta_{air}$ )) AS A FUNCTION OF FREE-SPACE BEAM DIAMETER, FOR THREE DIFFERENT COUPLING CONSTANT VALUES AT 1550 nm



4/17

**FIG. 7**

$n = 1.45$  FOR EVANESCENT LAYER

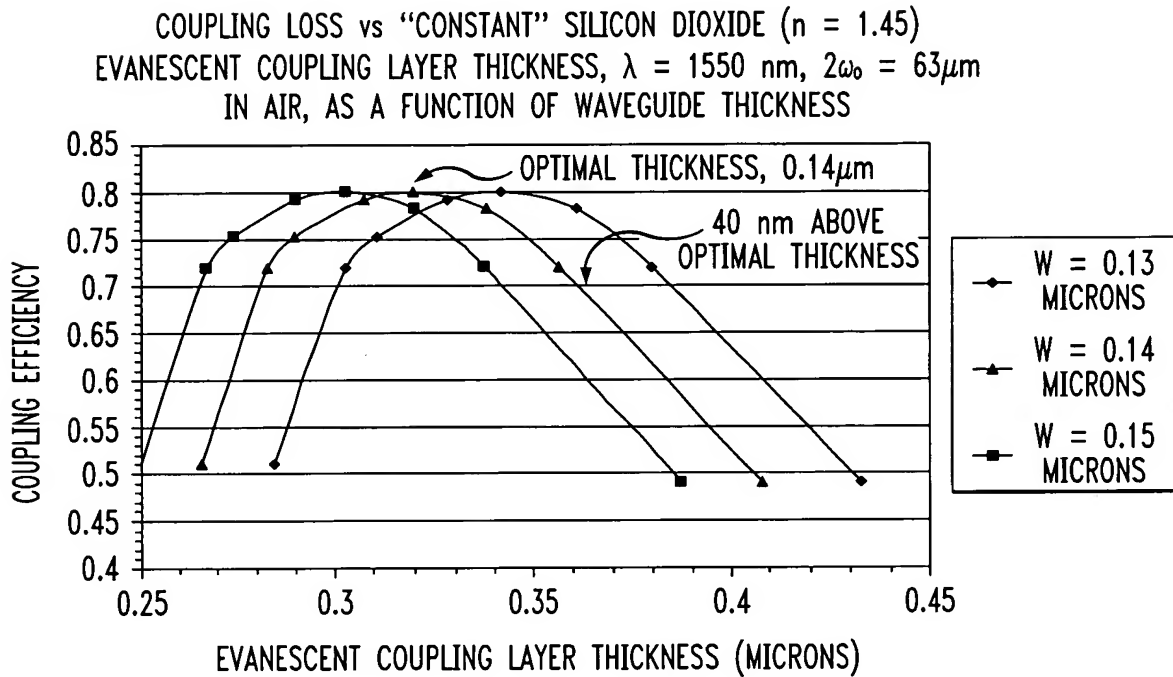
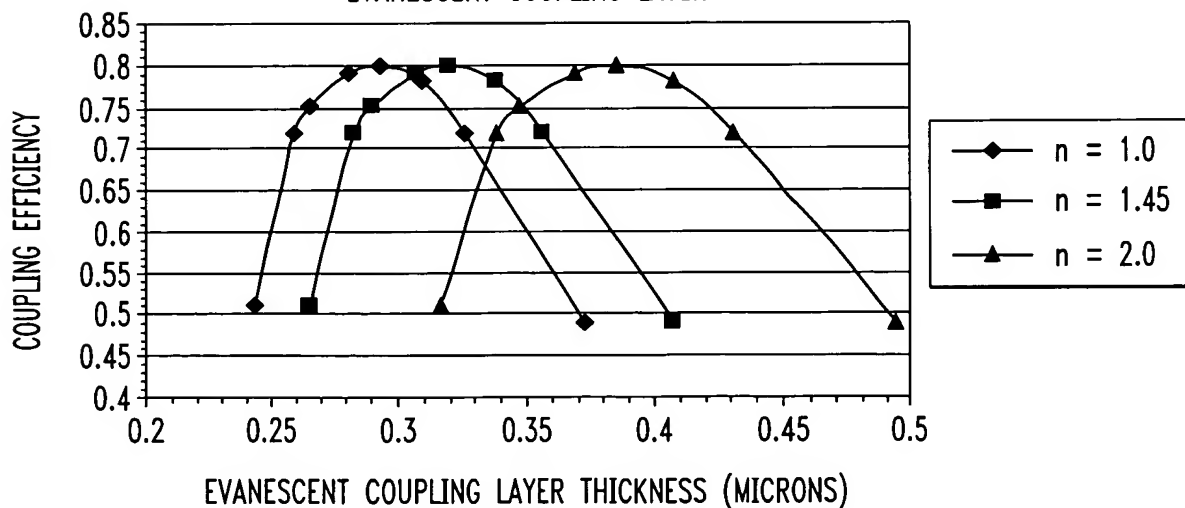


**FIG. 8**

COUPLING EFFICIENCY vs EVANESCENT COUPLING LAYER  
 THICKNESS,  $\lambda = 1550$  nm,  $2\omega_0 = 63\mu\text{m}$ ,  $W = 0.14\mu\text{m}$ , FOR  
 THREE DIFFERENT REFRACTIVE INDEX VALUES OF THE  
 EVANESCENT COUPLING LAYER



5/17

*FIG. 9*

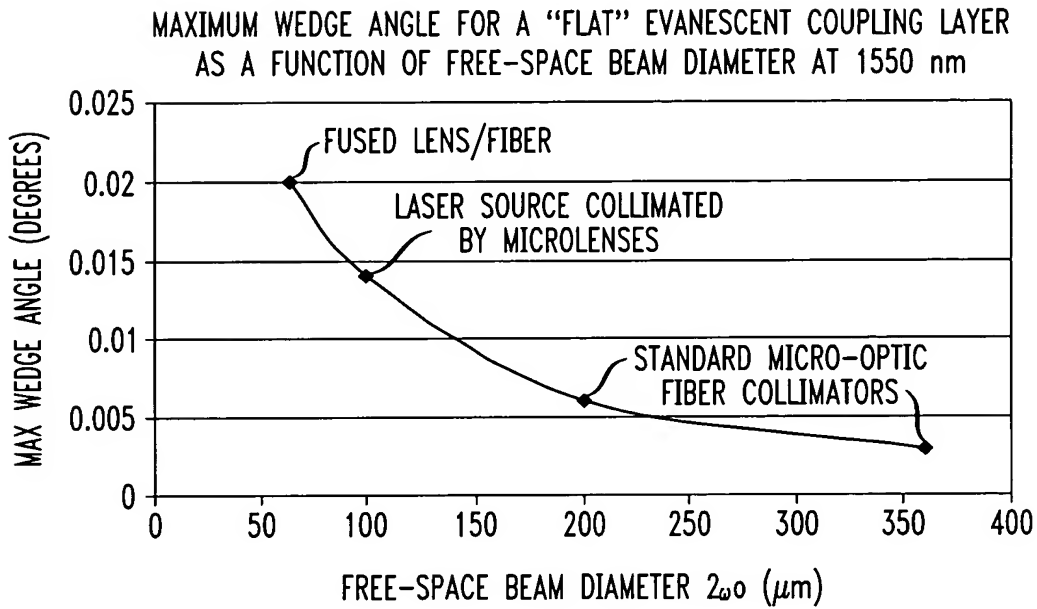


*FIG. 10*

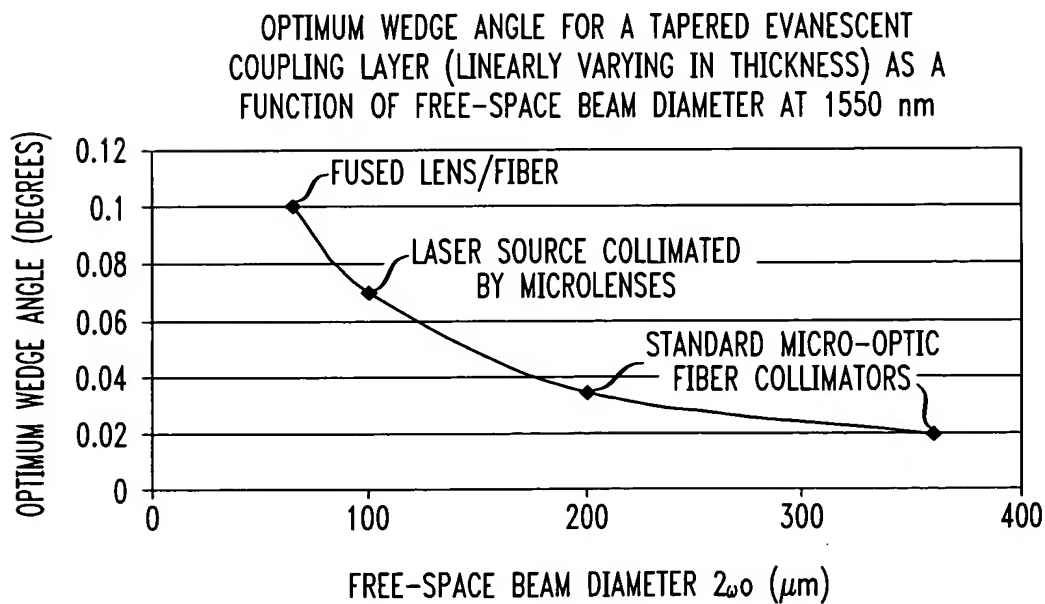
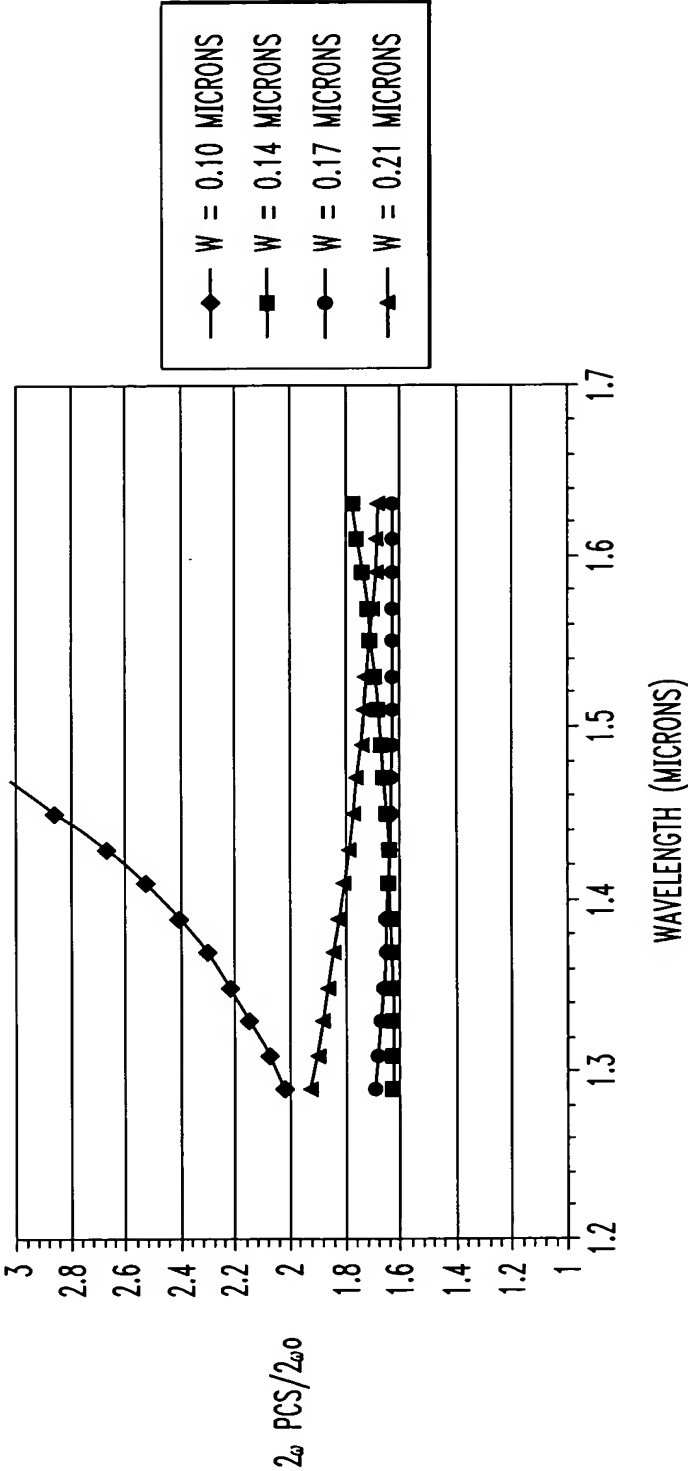


FIG. 11

GRAPHS OF  $2\omega_{PCS}/2\omega_0 = \{1 - (\sin\theta_{air}/n_{Si})^2\}^{1/2} \{\cos\theta_{air} * \cos\theta_{Si}\}$

RATION OF PROJECTION OF INPUT BEAM ON PRISM COUPLING  
SURFACE TO FREE SPACE BEAM SIZE, AS A FUNCTION OF  
WAVELENGTH FOR 4 DIFFERENT WAVEGUIDE THICKNESSES OF THE  
EMBODIMENT SHOWN IN FIGURE 2.1, WITH  $\theta_{pr} = 54.74$  DEGREES



7/17

FIG. 12

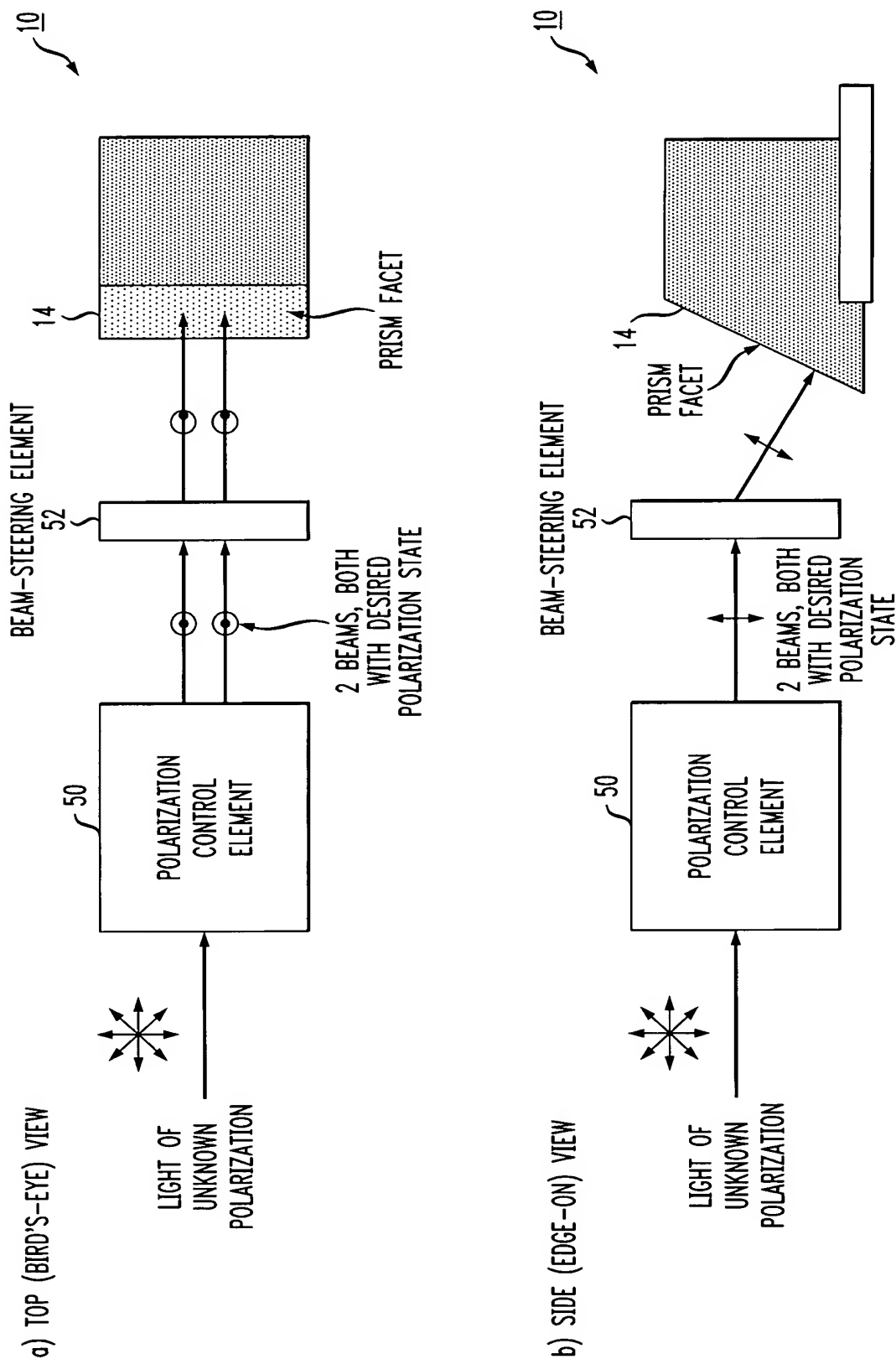
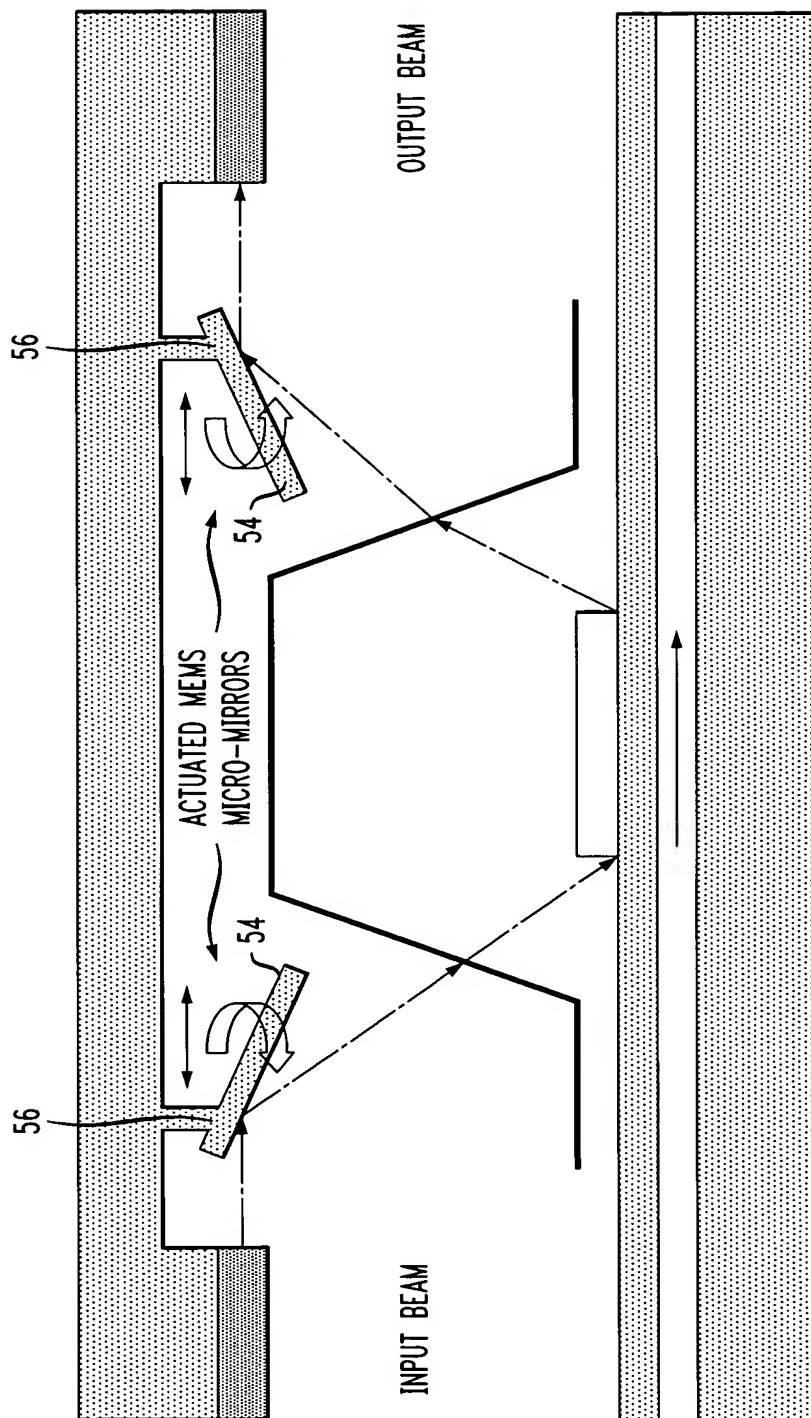


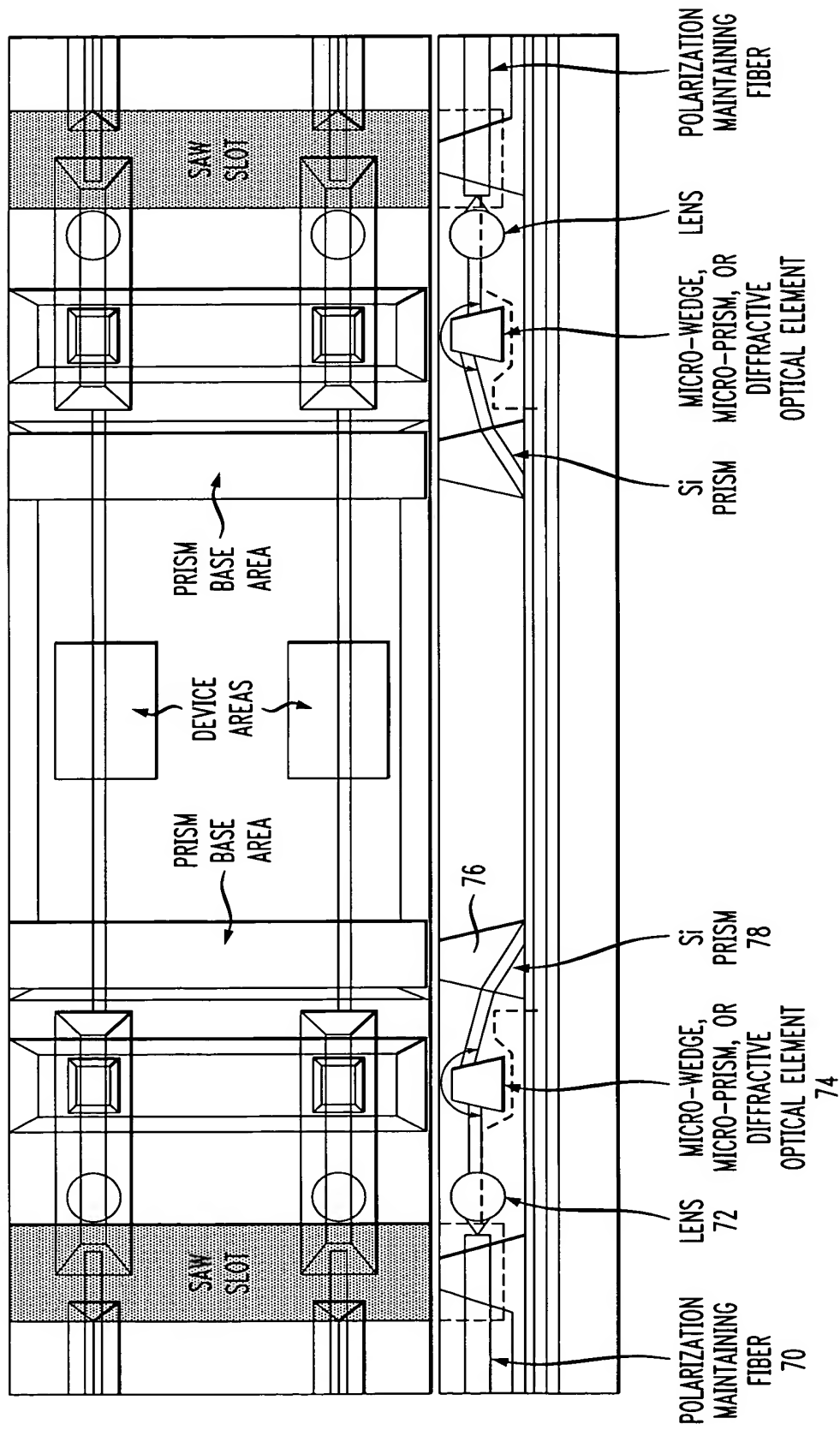
FIG. 13





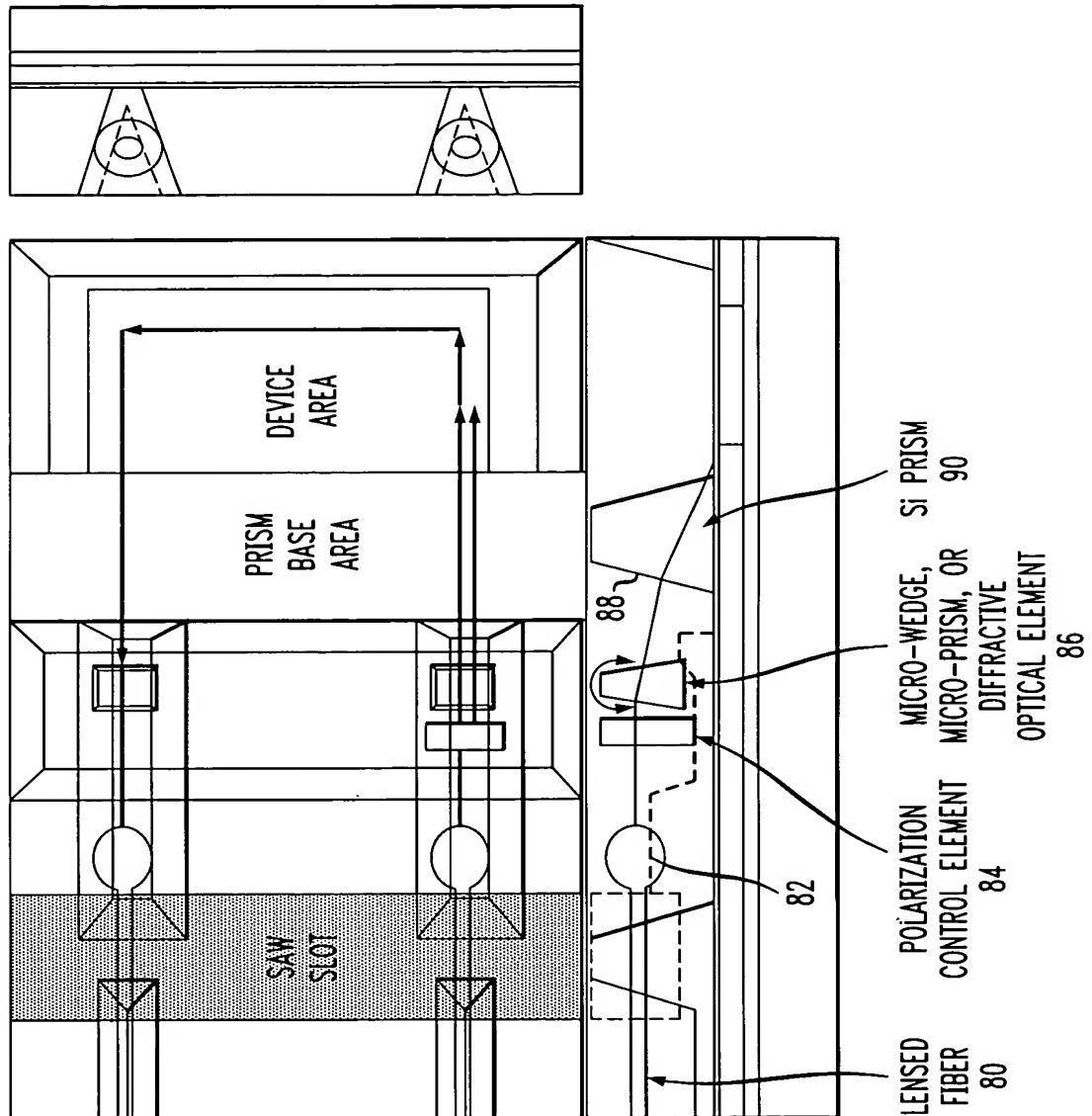
9/17

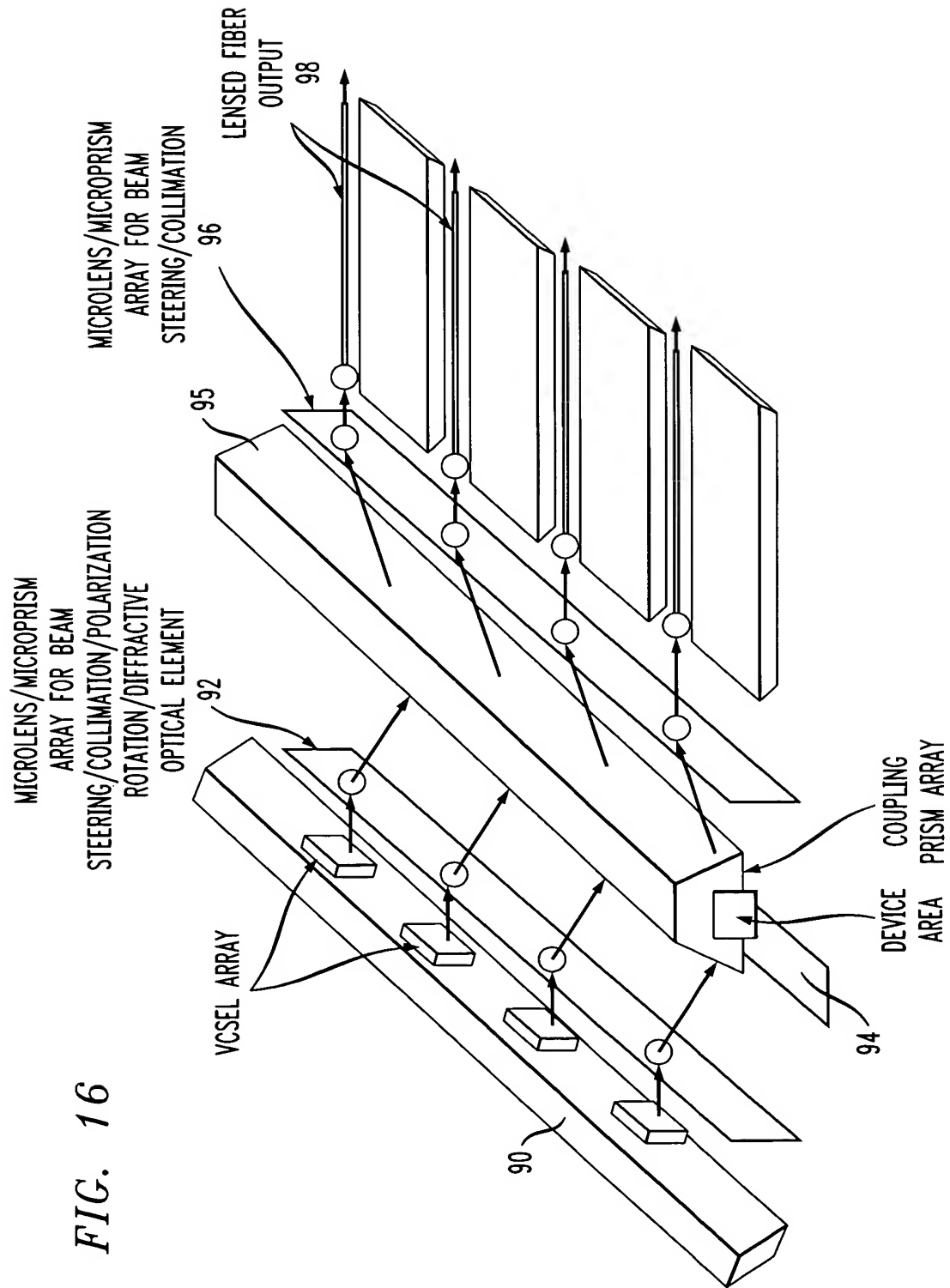
FIG. 14



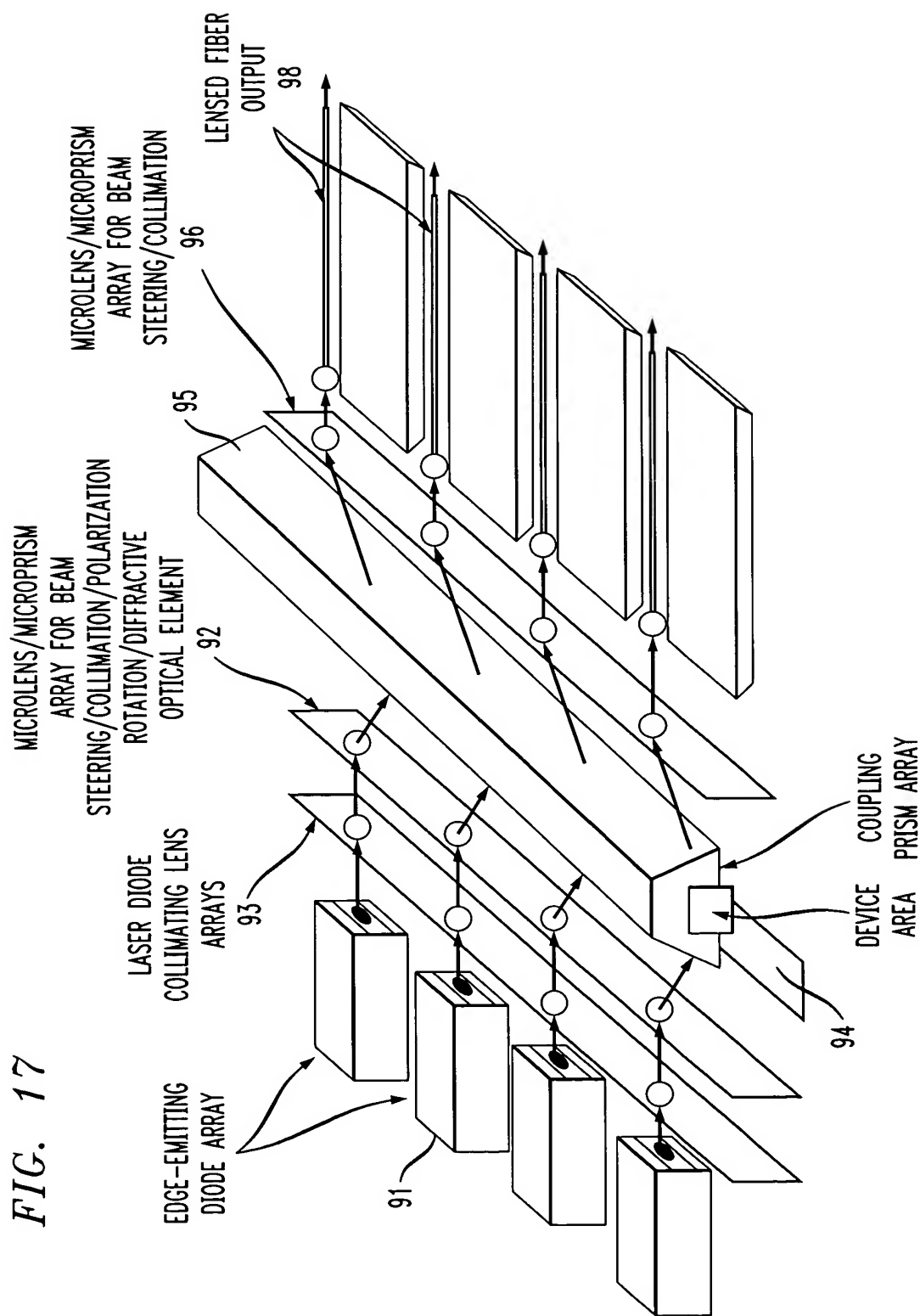
10/17

FIG. 15





12/17



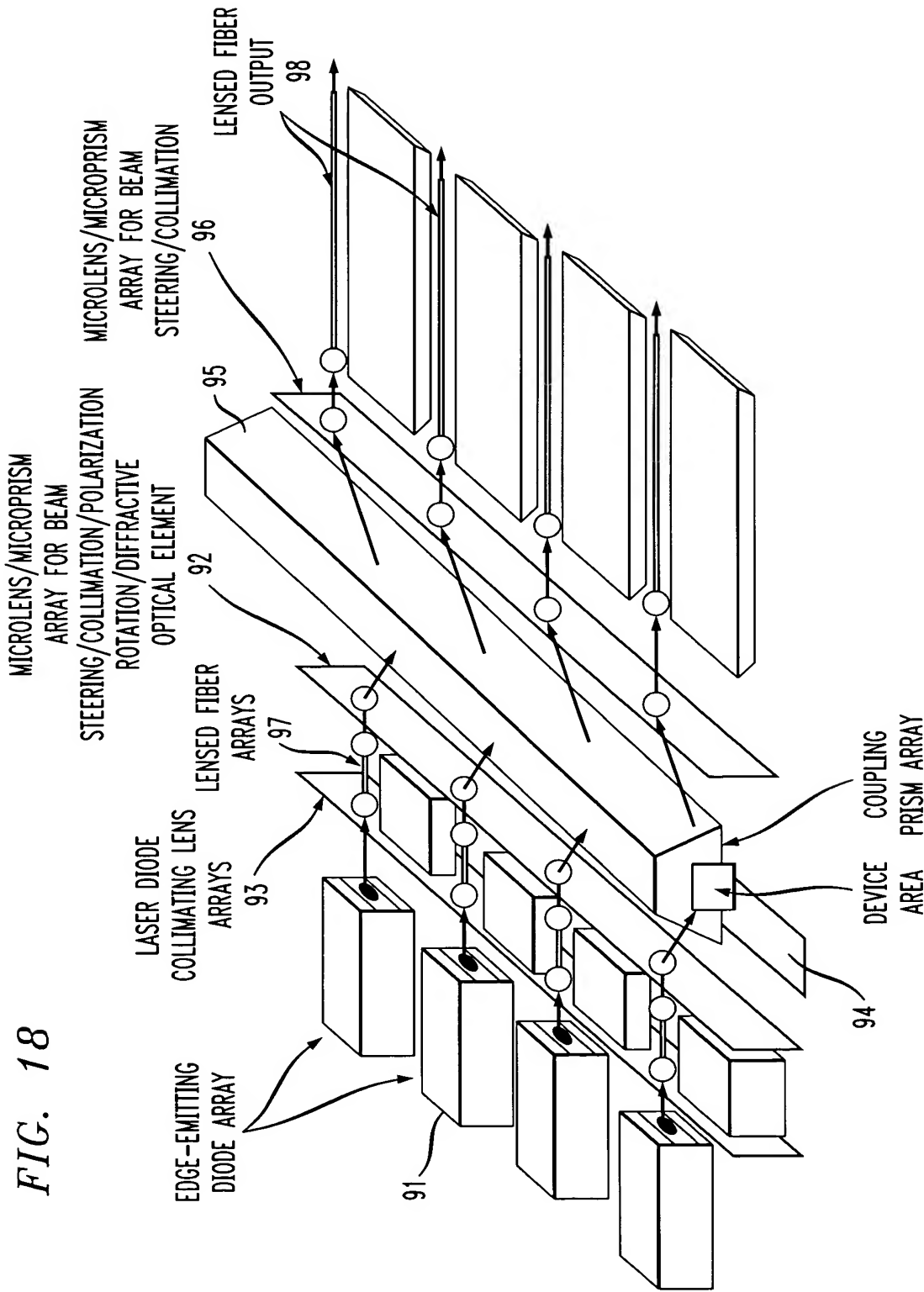
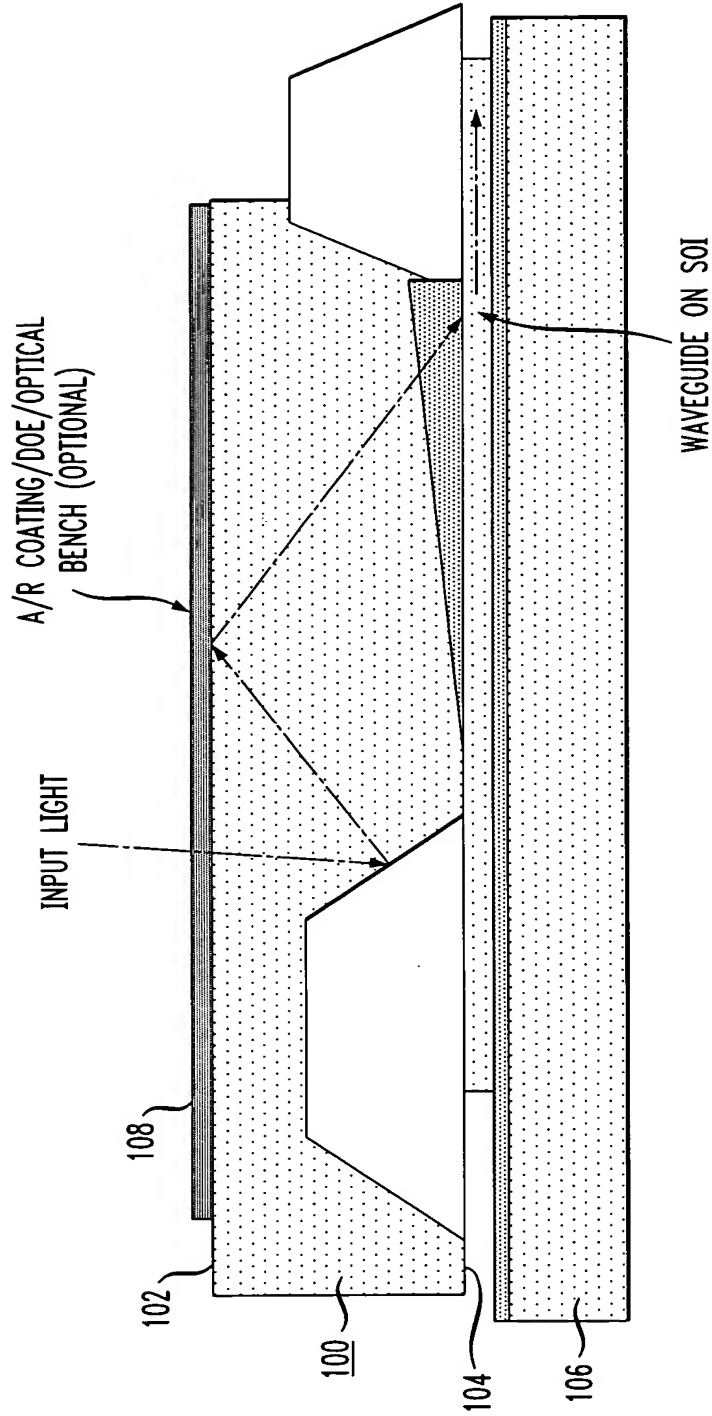


FIG. 19



15/17

FIG. 20

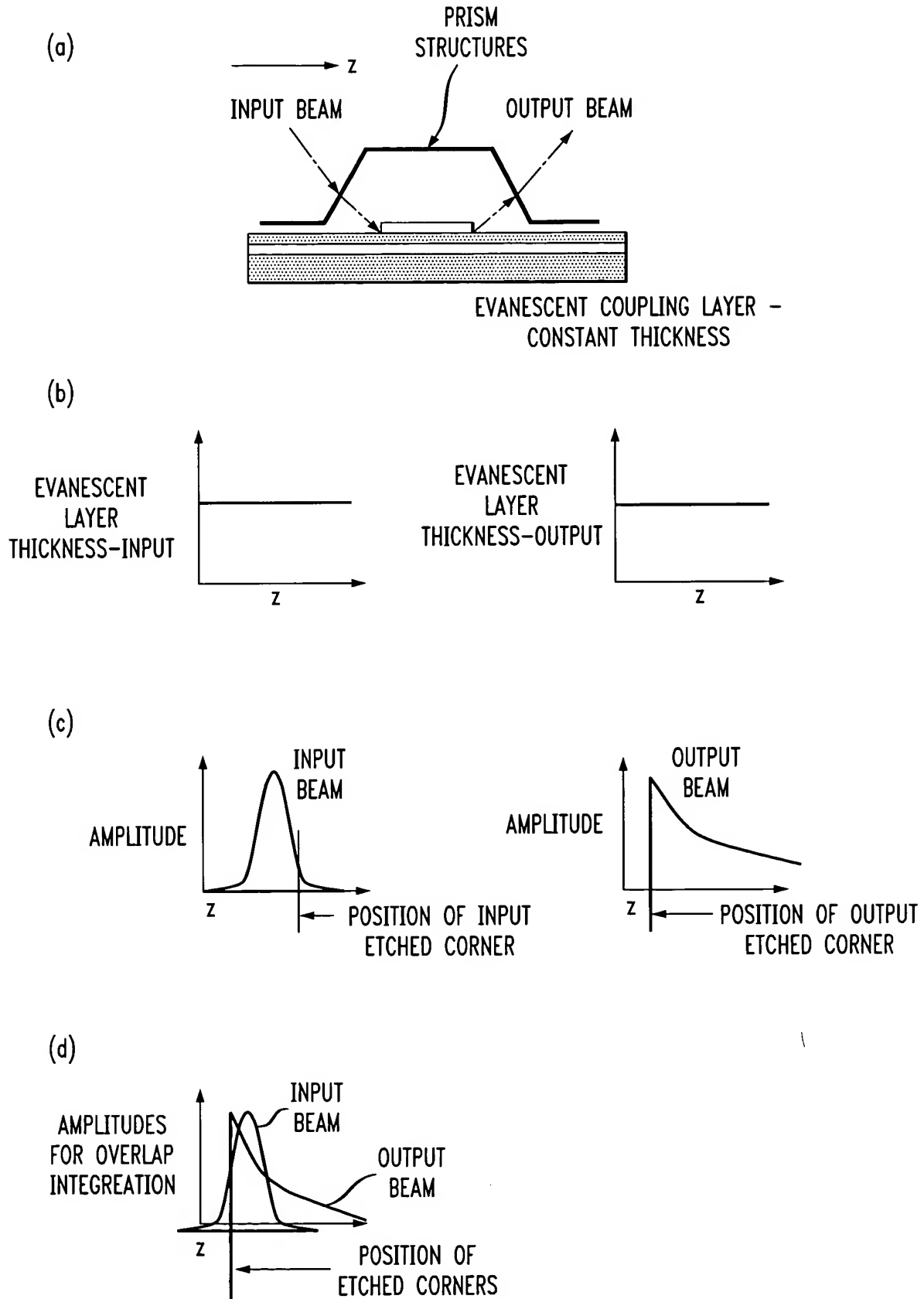


FIG. 21

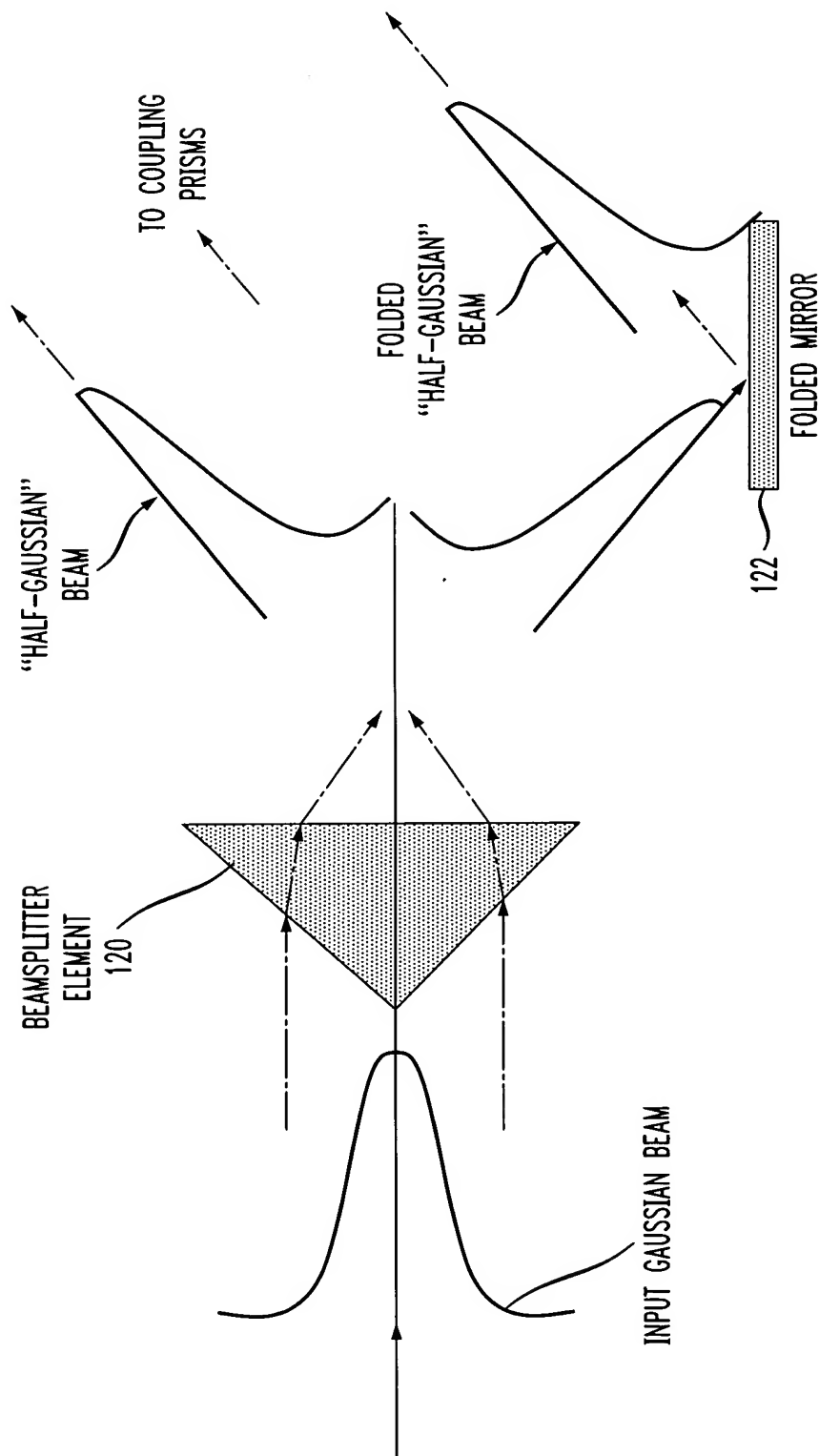




FIG. 22

